ELECTRICAL CHARACTERISTICS OF FROG ATRIAL TRABECULAE IN THE DOUBLE SUCROSE GAP

J. CONNOR, L. BARR, *and* E. JAKOBSSON

From the Department of Physiology and Biophysics, University of Illinois, Urbana, Illinois 61801

ABSTRACT The electrical behavior of small single frog atrial trabeculae in the double sucrose gap has been investigated. The currents injected during voltage clamp experiments did not behave as predicted from the assumption of spatial uniformity of the voltage across a Hodgkin-Huxley membrane. Much of the difference is due to the geometrical complexities of this tissue. Nonetheless, two transient inward currents have been identified, the faster of which is blocked by tetrodotoxin (TTX). The magnitude of the slower transient varies markedly between preparations but always increases in a given preparation with increase of external calcium. The fast transient current traces, at small to intermediate depolarizations, are often marred by the presence of notches and secondary peaks due most probably to the loss of space clamp conditions. In many preparations these could be removed by reducing the current magnitude through application of a partially-blocking dose of TTX. Conversely, in the preparations whose fast transient was fully blocked by TTX, notches and secondary peaks in the slow transient could be induced through increasing calcium concentration and thereby the slow current magnitude. Previously used techniques for the measurement of the reversal potential of the fast inward transient have been shown to be invalid. In so far as they can be measured, the reversal potentials of the fast and slow inward transient are in the same neighborhood, i.e. around 120 mV from rest. The true values may be quite a bit apart. The total charge flow in the capacitive transient was measured for different sized nodes and preparations. From these data and estimates of plasma membrane area per unit trabecular volume, specific membrane capacitances of around 3 $\mu F/cm^2$ were calculated for small bundles. The apparent ion current densities on this basis are approximately 1/10 of those measured in axons. The capacitive current occurring in small bundles decayed as the sum of at least three exponential functions of time. On the basis of these data and the anomalously large stable node widths, we suggest a coaxial core model of the preparation with the inner elements in series with an additional large extracellular resistance.

INTRODUCTION

A large number of studies on heart muscle have been carried out in which investigators have attempted to use voltage clamp analysis to identify and characterize the membrane currents underlying cardiac electrical activity. The thrust of much of the work has been toward identifying sodium and potassium carrying systems of similar nature

to those found in axons and establishing the existence of a transmembrane calcium flux during excitation. Unfortunately, these advanced studies have preceded a sound understanding of the passive properties of the preparations studied or equivalently stated, without a generally accepted circuit model for either mammalian or lower vertebrate preparations.

The voltage clamp technique itself, involving as it does the analysis of time and space varying potential profiles, has been rigorously defined only for relatively simple geometries such as single tubes and uniform spheres which have been used as idealized representations of axons and cell bodies, respectively (Cole, 1968). An approach to the problem of multicellular bundles such as cardiac tissue has been offered by Kootsey and Johnson (1972). The results of this study indicate that for cardiac muscle preparations the assumption of good voltage clamp conditions must be carefully justified and that in most previously published studies the necessary control has not been substantiated.

A number of investigations of voltage homogeneity in the test region of a single or double sucrose gap have been attempted by making use of a roving microelectrode to sample the voltage between the bath and various intracellular points. Reporting findings have been variable, some studies indicating negligible voltage variation in single cells in the test region in the period following the capacitive surge (New and Trautwein, 1972; Haas et al., 1971), others indicating much larger variations (Giebisch and Weidman, 1971; Beeler and Reuter, 1970). Negative evidence from microelectrode studies is certainly indicative of the failure of membrane voltage space clamp, but because of external series resistance, a voltage measured by an internal microelectrode is not necessarily only a transmembrane voltage (c.f., Beeler and Reuter, 1970; Kootsey and Johnson, 1972); therefore, positive results (apparently good voltage controls) are not uniquely interpretable. External series resistance is the resistance of the medium lying between the exterior of a cell surface and the grounding point of the bathing solution. This parameter is a function of tissue geometry and probably varies markedly depending upon the location of a particular cell in a bundle. The total voltage seen by an intracellular electrode is then the sum of the membrane voltage and any IR drop across the extracellular resistance.

Despite the diversity of clamping techniques and tissue bundle geometries which have been employed in various studies and the many possible ways in which artifacts can arise, the rather surprising fact remains that nearly all the voltage clamp studies aimed at studying the inward membrane current have produced essentially the same findings. That is, capacitance charging time is long and there are two components of transient inward current, an early, fast one carried by sodium and a slower one, the magnitude of which depends on the concentration of calcium in the bath. However, straightforward interpretations of the experimental results have not achieved widespread acceptance because of the lack of an adequate theoretical description of the experimental situation.

The study reported here was undertaken for three purposes: (*1*) to investigate the extent to which currents in frog atrium in voltage clamp experiments correspond to

axonal membrane currents, especially under conditions of known voltage inhomogeneity, as in the Taylor et al. study (1960); (*2*) to explore passive electrical properties and changes in these properties with preparation size in order to aid in the development of an electrical model of the tissue suitable to analysis; (*3*) to explore the ionic identity of the current carriers. A companion article will present computations based upon a simplified form of the model and standard squid axon sodium current parameters (Jakobsson et al., 1975). Some results have been given in preliminary reports (Connor et al., 1973; Jakobsson et al., 1974).

MATERIALS AND METHODS

Experiments were performed on single atrial trabeculae approximately 4 mm long from frog (*Rana pipiens, pipiens,* and *Rana pipiens, Berlandieri*). The most satisfactory bundles were 40–80 μm in diameter and free of any cross connections with the atrial wall or other trabeculae for 2–4 mm. The preparation was removed from the heart, generally from the left atrium near the pacemaker, by trimming out small chunks of muscle from the wall at each end of the trabecula. These endpieces served as mounting points in a double sucrose gap recording chamber. The end compartments of the chamber, voltage, and current pools, were isolated from the sucrose cuffs by Vaseline seals. The test node was formed by the interfaces between the sucrose cuffs and the central saline stream with no intervening partitions (c.f., Julian et al., 1962*a*; Nakajima and Bastian, 1974). The interfaces were clearly visible and lengths were measured at 60 × magnification. At the flow rates required, the test node width could be varied from about 70 to 700 μm. The region between end pools was sealed over with a glass cover slip. This sealed chamber had the advantage of giving a very stable test node and also eliminated the need for suction points. The end seals permitted a higher pressure to be maintained in the center chamber than if the ends were open. There was good correlation between action potential height and this pressure (or flow rate); low pressures led to smaller observed action potential. Presumably, washout of ions from the extracellular space under the sucrose cuffs was better at the high flow rates. Input resistance looking from the voltage end pool to ground was monitored by injecting current (500 Hz square wave, 1 nA peak to peak) into the voltage pool and measuring the step portion of the voltage change at that same point. Input resistance in excess of 5 MΩ indicated excessive damage or partially discontinuous bundles.

In several larger preparations transmembrane voltage in the test node was monitored simultaneously by a standard intracellular microelectrode (tip resistance 40–100 MΩ). The electrode was introduced into the chamber through a lateral hole and the seal maintained by means of a moveable cuff.

The electronic circuitry is of standard form (c.f., Connor and Stevens, 1971; Julian et al., 1962*b*). Transgap voltage, the potential between the voltage pool and the test node, was monitored differentially. All amplification stages employed Teledyne-Philbrick Model 1026 operational amplifiers (Teledyne-Philbrick, Dedham, Mass.) except the voltage head stages which were constructed from GPS Model 9504 operational amplifiers (GPS Corp., Farmingham, Mass.) mounted near the chamber. High frequency response of the head stages could be adjusted through positive feedback to give a 20 μs rise time with a 5 MΩ resistor connected from input to ground and a square wave signal injected at the input. The open loop frequency response of the voltage control circuit was flat to 250 kilocycles. The maximum open loop gain was 2,000 × . The apparatus was "bioassayed" by clamping lobster giant axons and matching published results from these preparations (Julian et al., 1962*b*).

Because of the uncertain nature of resting potential measurements in the sucrose gap, voltage levels in a given experiment are referenced to the preparation resting level.

Standard physiological saline was 100 mM NaCl, 1.9 mM KCl, 1.1 mM $CaCl_2$, 5 mM Tris. Tetraethylammonium chloride (TEA) at a concentration of 10 mM was used to reduce the delayed outward current (Rougier et al., 1968) in voltage clamp runs. Isotonic sucrose (75 g/liter) was deionized by filtration through an ion exchange resin (Amberlite MB-3, Mallinckrodt, St. Louis, Mo.) until a conductivity of less than 0.5 μmho/cm was attained. Exposure to air was limited during storage in the experimental vessels so that the conductivity never increased to above 1 μmho/cm. Experiments were done at approximately 15°C and at a pH of 7.4.

RESULTS

Action Potential Characteristics

Two sets of action potential records are shown in Fig. 1. In Fig. 1 *A* simultaneous transgap and microelectrode recordings are shown. The microelectrode tip was located near the current pool side of a 200 μm node. The amplitude of the microelectrode record is somewhat smaller than the transgap record but the time courses are otherwise nearly identical. In the best penetrations near equality of the action potential height in the two records was obtained but only for a very brief period (seconds) after which the penetrated cell suffered a loss of resting potential and action potential height,

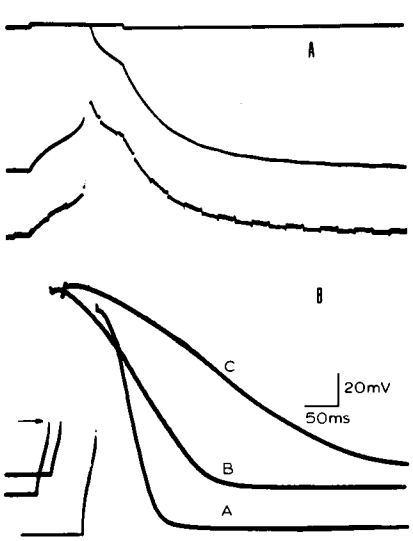

FIGURE 1

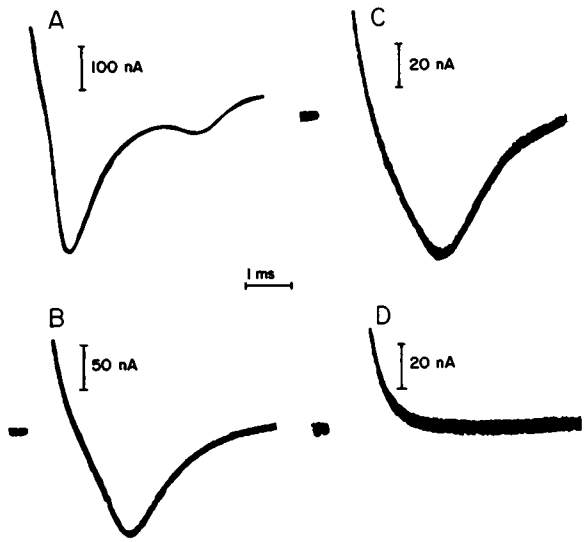

FIGURE 2

FIGURE 1 (*A*) Simultaneous records of transgap action potential (upper) and microelectrode recording (lower). Stimulus current is shown in the top trace. (*B*) Action potentials recorded at three different levels of applied backing current. Curve A, 0; curve B, 25×10^{-9} A; curve C, 30×10^{-9} A. The action potentials were evoked by pulses which terminated at, or slightly before, the fast upstroke phase. Arrow marks approximate position of threshold.

FIGURE 2 Four identical voltage clamp steps and the associated currents with preparation exposed to different concentrations of TTX. *A*, control; *B*, 5×10^{-9} M; *C*, 1.2×10^{-8} M; *D*, -3×10^{-6} M. Note changes in current sensitivity.

generally severe. The amplitude of the transgap action potential was the upper bound for electrode records.

The largest resting potentials measured from trabeculae mounted in the chamber ranged between 60 and 70 mV with no sucrose flow. Action potential height could not be measured in this condition because of muscle contraction. Maximum resting potentials in the node after sucrose flow had been started ranged between 80 and 110 mV. This hyperpolarization was first reported by Julian et al. (1962*a*) in the lobster giant axon. The presence of a sizeable hyperpolarization is also indicated in the transgap action potential records by the fact that threshold is often as much as 50 mV more positive than the rest potential, see Fig. 1 *B*, curve A.

When the sucrose gap hyperpolarization is nulled out by an applied backing current, action potential duration increases (Fig. 1 *B*, curves B and C). This shortening effect of hyperpolarizing current on cardiac action potentials has been reported for mammalian papillary muscle by Cranefield and Hoffman (1958).

The amplitude of the action potentials recorded in the sucrose gap chamber, after taking into account the resting hyperpolarization, is well within the range recorded by microelectrodes in other reports (c.f., Hutter and Trautwein, 1956) whether transgap or microelectrode measure is used. In this situation we made the conservative estimate that the extracellular sucrose resistance is at least 10 times the total internal resistance of the bundle and therefore the extracellular sucrose shunt is more than 15 MΩ in our experiments.

We have not pursued a microelectrode investigation of voltage homogeneity in the clamped test node. Preparations which are even moderately favorable for microelectrode impalement in our present chamber are large, 80–100 μm diameter, and it is difficult for a number of reasons to set up a node as narrow as we consider desirable, 70–100 μm with the electrode present. The problem of maintaining a stable penetration for any length of time was mentioned earlier. The rapid damage to penetrated cells is probably due to the non-ideal conditions, for microelectrode recording, of our chamber. The muscle bundle hangs unsupported for a length of 2.5 mm in fast flowing streams of fluid and although no motion is detectable by microscope observation (60 ×) there probably is some, especially if an action potential is evoked. Also the axis of the microelectrode is normal to the bundle axis instead of a more favorable acute angle.

The observations we have made with simultaneous microelectrode recordings, however, have led us to favor the hypothesis that the transgap voltage and the injected current are useful measures of membrane properties.

Time Courses of Currents During Voltage Clamps

A basic assumption is that our trabeculae are in fact single functional electrical units. Some support for this was given by the observation that if two clearly demarcated trabeculae were placed in the sucrose gap, two clearly distinguishable action potentials were usually elicited, as compared to the one normally seen from one trabecula. Also, thin strips of muscle from the rather amorphous wall region gave multiple-response

patterns and highly irregular current patterns for small voltage clamp steps. These electrical cues were often evident in fibers of unitary outward appearance so that the selection of a suitable preparation was not always a routine matter. If much bulkier preparations were employed than we have used, it is quite probable that these irregularities in the measured current time courses would be smoothed by the averaging of a number of these signals each having a slightly different time course (Tarr, 1971). Many of the obvious features of electrical discontinuity can be eliminated in most cases by the careful selection of small, free-standing trabeculae. Given that such a preparation consists of cellular subunits whose internal electrical coupling is relatively close, the core conductor network still would have a relatively high internal resistance. We therefore imagined that any artifacts of poor voltage control would be similar in nature to, if more severe in magnitude than, those associated with the squid axon and investigated by Taylor et al. (1960). The important features of such artifacts are that they are exaggerated by low longitudinal conductance and by high transmembrane currents (in fact the appearance of the artifacts can be correlated directly to the product of peak current times the axial electrode resistance [(Cole, 1968]) and are by far most clearly evident at voltages corresponding to negative differential resistance in the voltage vs. peak sodium current curve.

"Abominable notches" (Cole, 1968) on the early inward current traces from our trabeculae appear and behave much as do the notches in curves from poorly controlled squid axons. That is, they are more exaggerated in traces from preparations with large peak inward current and they appear only in the negative resistance region of the voltage-current curve. Fig. 2 shows records of the early transient current at control conditions, 2 *A*, and at dosages of TTX which partially block this current, 2 *B* and *C*. It may be seen that notching disappears at the smaller currents and also that the time course of the rapid transient becomes slower in the more heavily TTX-dosed situations. In Fig. 2*D* the early transient has been completely blocked. Thus, there seem to be no fast channels unaffected by TTX.

The absence of notching in the current trace does not insure that spatial control is complete. However, one would expect that in the range of good control the time courses of the current traces for different TTX concentrations would be the same, the currents differing only by a scale factor. Fig. 3 shows the time-to-peak current for each of the three concentrations of TTX. It may be seen that the partly drugged states superimpose on each other and display a strong dependence on voltage. On the other hand, the peak time of the undrugged fast transient is clearly less, even in the positive resistance region, and it displays the marked independence of voltage that is expected of a poorly clamped preparation from squid studies.

Notching in the current traces can not only be removed by reducing current density but can be induced by increasing it. Although impractical for the fast Na transient, this can be done using the TTX insensitive transient described for this preparation by Rougier et al. (1969) and by Tarr (1971). The latter component of inward current has a relatively slow time course and small amplitude compared to the early transient and its magnitude changes with external calcium ion concentration. Fig. 4 shows the re-

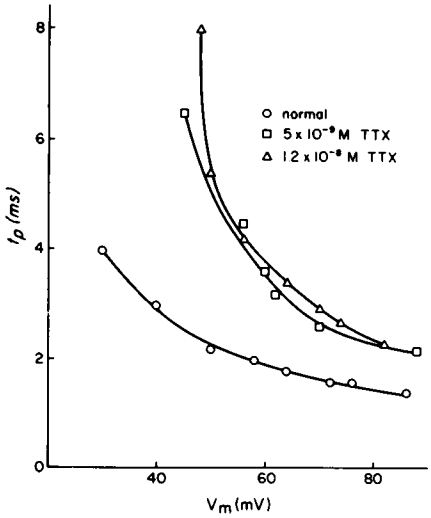

FIGURE 3

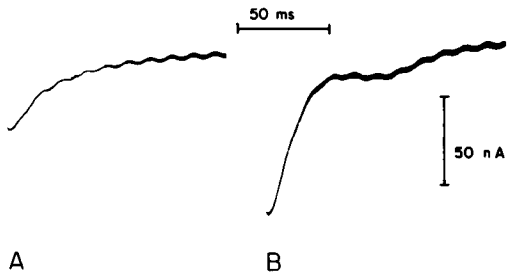

FIGURE 4

FIGURE 3 Time to peak of the early transient for control and two partially blocking dosages of TTX. Values are from the same data as Fig. 5.

FIGURE 4 Slow transient current (TTX insensitive). *A*: [Ca] = 1.1 mM; *B*: [Ca] = 4.4 mM. Notch present on decay phase of current in *B*.

sults of increasing external calcium concentration in a preparation exposed to 3×10^{-7} M TTX, which completely blocked the early, fast transient. In Fig. 4 *A* the calcium concentration was the normal value and in 4 *B*, four times normal. The voltage steps were approximately equal. Notching is clearly evident in the record of 4 *B* where the current magnitude is larger.

I_p-V Relationships

The relationship between the peak current and clamp voltage is of great physiological interest. Fig. 5 *A* shows the peak current-voltage curve for the early transient system of the trabecula, discussed in connection with Figs. 2 and 3, at various TTX dosages. Fig. 5 *B* shows these same currents normalized to the same peak value. It may be seen that there is a large voltage-shift on the negative-resistance limb when a partially-blocking dose of TTX is applied, but not much of a further shift when the dose is increased. We infer from these data that for the undrugged membrane the voltage clamp is quite unstable and control is poor in the negative resistance voltage region. Although all three curves nearly superimpose on each other in the positive resistance region, we are skeptical of voltage control of the undrugged membrane even in this region because, as is shown in Fig. 3, the time to peak is relatively independent of clamp voltage.

A plot of peak slow inward current vs. clamp voltage for the experiment discussed in Fig. 4 is given in Fig. 6. Note from this figure that the test step applied in Fig. 4, approximately 75 mV, fell in the negative resistance region of the I_{peak} vs. V_m curve.

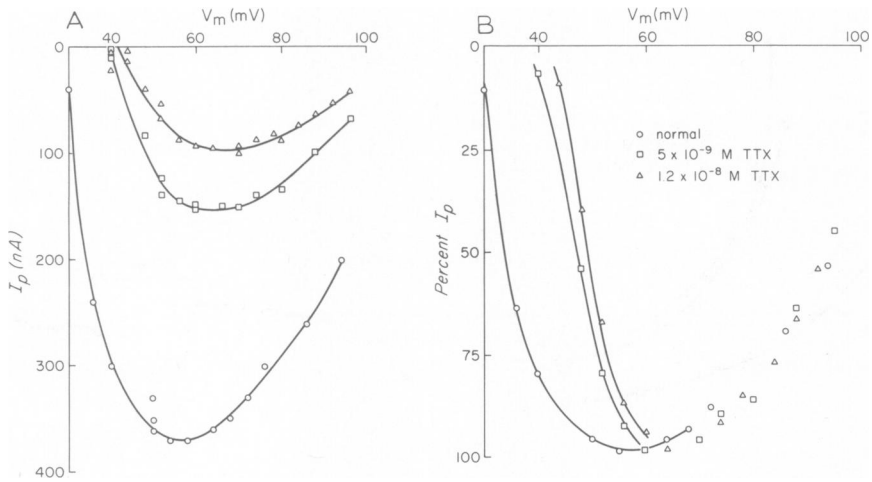

FIGURE 5 Plots of peak early transient vs. membrane voltage for a control and two partially blocking dosages of TTX. *A*, currents drawn to scale; *B*, each set of currents normalized to its maximum value.

Presumably the reason for the marred current pattern of 4 *B* is the greater slope of the I_{peak} vs. V_m curve at the higher calcium concentration.

Notching was never as severe a problem with the slow transient as for the fast. There are two possible contributing reasons for this. First, the observed current densities of the slow transient are uniformly much smaller than those of the fast transient. Second, the negative resistance part of the I_p vs. V_m curve, insofar as we can measure it, is steeper for the fast than for the slow transient, covering a region of approximately 25 mV for the fast transient and 40 mV for the slow transient. In no case, however, do we see a negative resistance region of the V_m vs. I_p curve as steep as that for the fast transient in dog ventricular trabeculae reported by Beeler and Reuter (1970). A feature of Figs. 5 and 6 which should be emphasized is that there are no obvious cues in the shape of the curves to correspond to the clearly artifactual patterns in the raw data from which they were constructed.

The magnitude of the TTX-insensitive inward transient was greatly variable from one preparation to another. In some preparations, this current component could not be seen in normal calcium concentrations, but did appear when higher concentrations of calcium were used in the bathing solution. Note that the observed peak slow current tends to saturate with increased external calcium (Fig. 6).

Reversal Potential for the Fast Transient Current

The fast current transient disappears in the absence of sodium ions and is sensitive to TTX. Because of the very specific action of tetrodotoxin on the sodium conductance mechanism (Narahashi et al., 1964; Hille, 1968) its use has become a standard technique for determining the time course of the sodium current and its reversal potential. Fig. 7 shows companion sets of voltage clamp records made in normal Ringer's and in

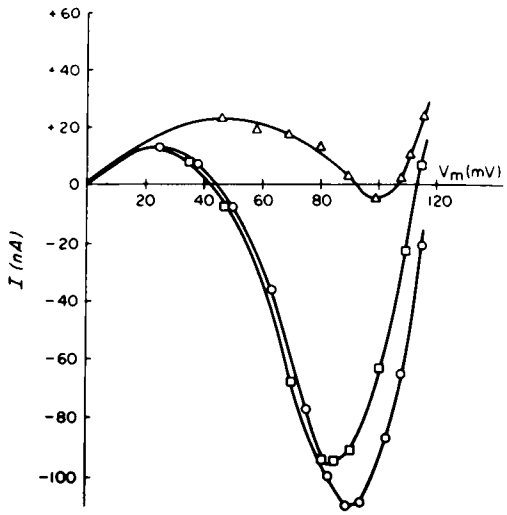

FIGURE 6

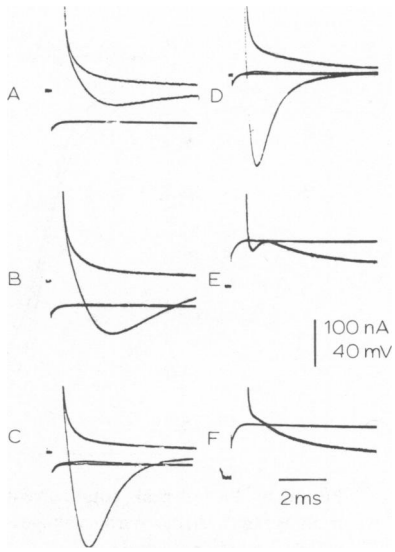

FIGURE 7

FIGURE 6 I_p vs. V_m relations for TTX insensitive (slow) transient at three levels of external calcium. △, [Ca] = 1.1 mM; □, [Ca] = 4.4; ○, [Ca] = 8.8.

FIGURE 7 A thorough series of voltage clamp records. In *A*, *B*, *C*, and *D* are shown superimposed records of currents taken in normal Ringer's and in Ringer's containing 5×10^{-7} M TTX. The test voltage level appears in each frame; the holding voltage is off scale. Only control currents appear in the last two frames (*E* and *F*) because TTX runs were not made at exactly these voltages.

Ringer's to which a blocking concentration of TTX has been added. If currents corresponding to identical voltage steps are subtracted, the remainder is presumably the isolated sodium current. The point at which a plot of peak sodium current crosses the positive limb of the membrane voltage axis is the reversal potential. In theory this procedure should be applicable in determining the reversal potential for the early transient in atrial trabeculae, if one has achieved adequate space clamp. In practice the results are difficult to interpret since, by this method, the apparent reversal potential for the early current is unreasonably high (see Fig. 8) or the time course of the difference current does not show a peak beyond a certain voltage.

Two types of explanations are possible for this behavior. The first, and one we tend to reject out of hand, is that TTX is activating a transient outward current; the current would have to be transient because the companion current waveforms, undrugged and drugged, ultimately converge. The second explanation (see also Beeler and Reuter, 1970) is that the transmembrane voltage of some significant population of cells in the test node is not under good control. In normal saline these cells would constitute a source of inward current, which, while not giving a notch, could at least decrease the membrane capacity charging time course. For large voltage steps this charging time clearly overlaps the developmental and peak phases of the early transient current. If

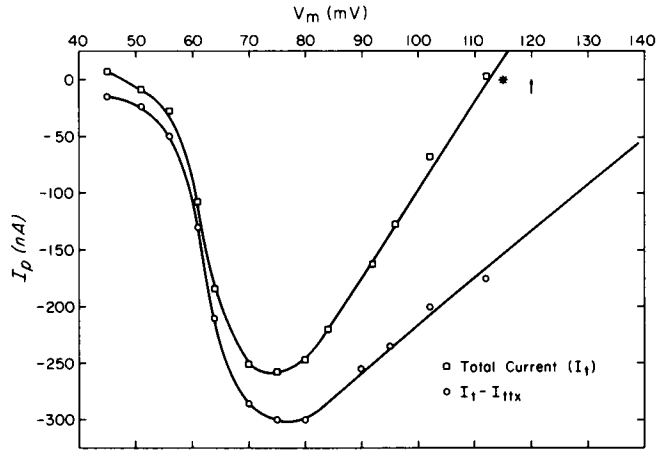

FIGURE 8 Plot of peak, total current, and separated current vs. V_m. Data from same experiment as Fig. 7. Arrow marks voltage at which early transient becomes outward flowing. Asterisk indicates action potential peak.

applied TTX blocks the early transient in all cells of the node, then the voltage control amplifier is faced with an added capacitance charging burden and the outward current it must supply during the first millisecond or two following a step voltage change is larger. Thus, the difference between companion currents, control and TTX blocked, would be expected to have an extra inward component and not go to zero at the actual reversal potential.

A second method of estimating the early transient equilibrium voltage is to note the voltage at which the early transient current changes directions from inward to outward (Fig. 7 *E* and *F*). A third and very approximate measure is to use the zero crossing of total current peak. This method must yield to a low reversal potential but avoids the error discussed above. The three measures have been applied to the data shown in Fig. 7 and the results plotted in Fig. 8. From these results one cannot define a reversal potential from the fast transient. Indeed, the estimate by the subtraction method puts the value well within the region found for the slow transient (c.f., Rougier et al., 1969; Tarr, 1971) and would seem to make this criterion an unreliable one for establishing differences in the ion species carrying the two currents.

On the face of it then, we have presented evidence supporting the idea that the electrical behavior of a bundle of cardiac cells is similar to that of a model system such as the squid axon with respect to the voltage clamp irregularities expected for high values of internal and extracellular resistance. These observations are favorable to the supposition that a strand of heart cells may be considered to be like a single axon with high internal and external series resistances. They are obviously not sufficient grounds for doing so. One needs a suitable model derived from the passive electrical characteristics of the preparation and its geometry. The following paper will consider this problem. It was found that reducing the membrane current improves only certain

aspects of the clamp picture but in particular does not improve the reversal potential measurements.

Transmembrane Current Density

Our data indicate that current density resulting from ion specific conductance changes in heart tissue is normally far less than that in axons. For example, in our experiments the total current of the early transient is about the same as one measures in a lobster giant axon or crustacean walking leg axon of the same outside dimension, 50–100 μm (Julian et al., 1962*b*; Connor, personal observation). There should be a large difference in the quantity of excitable membrane, however. We have determined a rough value for the amount of heart cell plasma membrane expected in the test node in the following manner. Montages approximating the cross-sectional dimensions of atrial trabeculae were laid out using electron micrographs (courtesy of Dr. Maynard M. Dewey) chosen out of a batch from a given sectioning block, each photograph covering approximately a 10 × 15μm area. The length of plasma membrane in the cross section was then measured. The small irregularities always present on the cell perimeters were not included in this length so that this measurement is an underestimate. For trabeculae of roughly 50 μm in cross-sectional diameter, the total measured length was approximately 15 times that of the circumference of a right cylinder of the same diameter. To compute area, we made the assumption that the cell cross sections in a montage were random so that total area was proportional to the test node width. Therefore, we would expect approximately fifteen times more membrane area in a trabecula than in an axon of the same diameter. This area ratio should increase as the square of bundle diameter. On this basis the early transient current never exceeded 100 μA/cm^2 and leakage resistances lay between 1 and 15 kΩ-cm^2 depending on the preparation and on which part of the *I-V* curve measurements were taken. Sample *I-V* curves run TEA and TTX Ringer's solutions are shown in Fig. 9.

An apparently low ion current density could be due to one of two causes. First, the

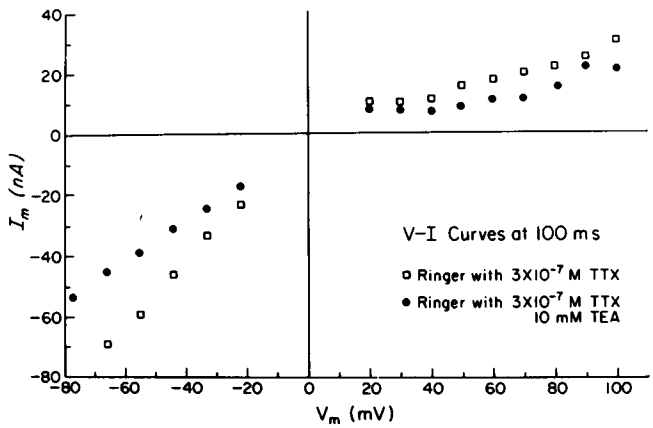

FIGURE 9 *V-I* curve taken at 100 ms following voltage step from rest (V = 0).

density of ion channels could simply be lower in heart muscle than in axon. The leakage conductance of assorted membranes, ranging from a few kΩ-cm^2 for squid axon to a few hundred Ω-cm^2 for some molluscan neural somata (Gorman and Mirolli, 1972) would certainly indicate that this is possible. Second, some of the plasma membrane in the node might not be participating properly in the sodium gating process. This in turn could be due to a series resistance large enough to make some regions "electrically less visible." There is no way of discriminating between these possibilities on the basis of conductance measurements alone.

Membrane Capacitance

Membrane capacitance, on the other hand, has proved to lie consistently in the range of from 1 to 2 μF/cm^2 (Cole, 1968). Therefore, we felt it worthwhile to determine whether there was a similar large discrepancy between the capacitance values of other membranes and values we could obtain from the integrals of the charging currents and the membrane areas estimated from electron micrographs. It should be pointed out that these cells have no T-tubular system (Barr et al., 1965; Staley and Benson, 1968).

Fig. 10 shows the initial current flow in response to a small negative step for preparations of two different sizes. All voltage steps in this section are $\pm$15 mV or less from the resting potential in order to avoid perturbing any time-dependent conductance changes. As has been discussed previously, this initial current persists after the voltage trace is essentially flat, indicating that there is a resistance in series with the membrane capacitance (c.f., Tarr and Trank, 1971; Fozzard, 1966). Regardless of the presence or absence of this series resistance, if the same voltage step has indeed been realized across all the membrane capacitance, then after the current surge has decayed to zero, the total charge Q, which has flowed should be given by $Q = Cm \cdot \Delta V_m$, where

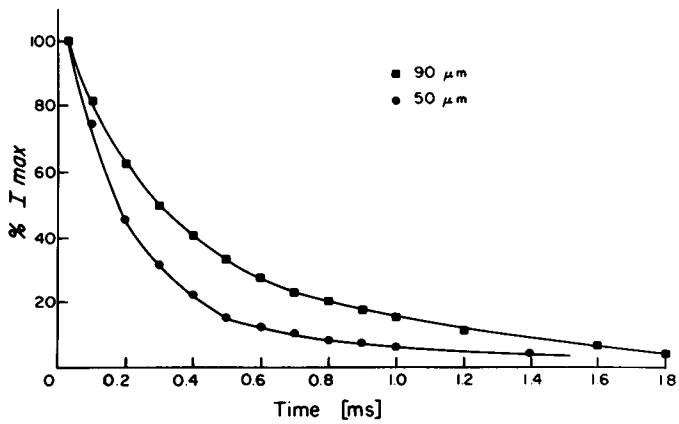

FIGURE 10 Initial current flow after a small voltage step in two bundles of different size. Currents shown normalized and inverted.

Cm is the total capacitance of the membrane in the test node and ΔV_m is the magnitude of the transmembrane voltage step (Adrian and Almers, 1974).

Using the data of Fig. 10, and assuming that the steady-state voltage drop across the extracellular resistance is negligible, the capacitance charged by the voltage-clamp circuit is 7.1×10^{-3} μF for the smaller preparation, an atypically low value, and 14.5×10^{-3} μF for the larger one. From our estimates of total membrane area and assuming a specific capacitance of 1 μF/cm^2 we could have expected a capacitance of 2.4×10^{-3} μF, and 7.6×10^{-3} μF. The capacitive transient was studied in 25 preparations which ranged in size from 40 to 120 μm in cross-sectional diameter. When the electrical (C_e) and geometrical (C_g) estimates for total capacitance were compared for each preparation, they differed by a factor of around 3. Additional values are given in Table I. Because of experimental factors which are difficult to control or measure, such as the degree of stretch of a mounted bundle, thickness of the sucrose-saline mixing regions at the node boundaries the degree of cell packing within the bundle and longitudinal folding, the figures given are not reliable estimates of true specific capacitance. In addition, the steady-state transmembrane voltage may decay with distance. However, the fact that the deviation from the standard 1 to 2 μF/cm^2 is on the high side would support the idea that in the steady state the bulk of node membrane is undergoing the voltage change imposed by the external circuitry, and that therefore the density of ion channels appears to be lower than in axon.

Previous studies have indicated that the capacitive transient decay is a single exponential process in frog atrial tissue (Rougier et al., 1968; Tarr and Trank, 1971). However, we have found that for small to medium-size bundles (< 100 μm diameter) and node width no greater than twice the preparation diameter, the capacitive decay is

TABLE I

ELECTRICAL PARAMETERS OF NODE

Preparation ident. and diameter	Node width	τ_1	τ_2	τ_3	R_s	R_m	C_E	C_E/C_G
	μM	ms			KΩ	MΩ	μF	
6271	60	0.13	0.5	4.2	70	1.8	5.5	3.9
D = 50	100	0.23	--	3.3	45	1.3	7.1	3
	150	0.26	--	--	34	0.8	10	2.8
6274	60	0.07	0.27	1.8	64	1.2	6.5	3.1
D = 60	100	0.13	0.65	3	56	1.4	11.3	3.3
	150	0.13	0.25	6	37	1	10.6	2.1
6272	100	0.21	0.93	10.1	39	0.7	10.5	3.1
D = 60	160	0.22	--	---	33	0.5	13.5	2.4
7241	66	0.175	0.75	5.4	99	1.1	12	4.4
D = 66	100	0.33	1.15	6.4	50	0.7	15	3.7
6273	60	0.18	0.65	2.4	73	1.3	14.7	4.6
D = 75	100	0.26	0.9	8.3	40	1	18.9	3.6
	200	0.6	--	11.5	29	0.41	26.8	2.5

-- indicates component not present.

best fitted by the sum of two to three exponentials (see Fig. 11). Only for node widths somewhat greater than twice the preparation diameter does the capacitive decay take on the appearance of a single exponential and then only over a restricted range of node widths (see Fig. 11). Time constant data are summarized in Table I along with estimates of the least series resistance ($R_s = \Delta V_m/\Delta I_{peak}$), total capacitance and membrane resistance ($\Delta V_m/\Delta I_{ss}$). The data show a good deal of scatter as one would expect from a preparation of this nature; however, a minimum of three exponentials was required to describe the capacitive transient in all but one or two cases. There was some tendency of the larger diameter preparations to exhibit longer time constants at node widths of 100 μm or less. In most cases, R_s decreased as preparation diameter increased.

Membrane resistance (R_m) for the table was measured from small negative voltage steps from rest potential. This method produced values of R_m which are smaller than those found by positive steps. Within the subthreshold voltage range, the larger the positive voltage step the larger the value of R_m is. As an example, the Table I entry, 7241, was tested with positive pulses of 13.5 mV and 34 mV. R_m values of 1.4 MΩ and 11 MΩ, respectively, were measured for a 100 μm node.

Total capacitance increased with node width but not in direct proportion in all cases. We would offer two probable reasons for this. First, at the smallest node widths the

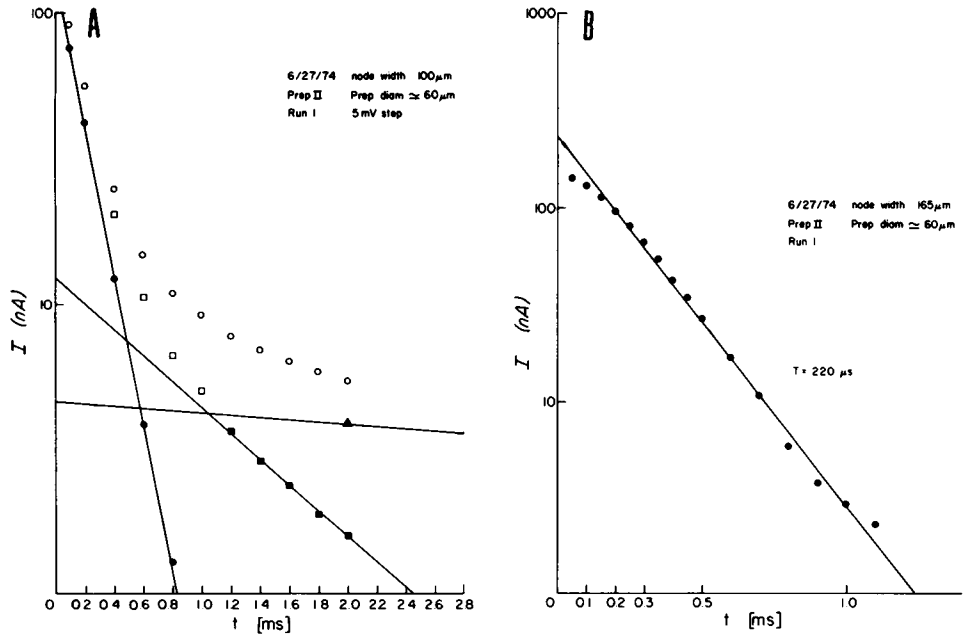

FIGURE 11 Semilog plot of the capacitive transient from a 60 μm diameter preparation (see line 4 in Table I). *A*: node width 100 μm. Three exponentials are required to fit data (open circles). The slowest component was derived from a separate plot. *B*: node width 165 μm. Data are approximately fit by a single exponential.

sucrose-saline mixing regions possibly constitute a sizeable fraction of the actual test node. Therefore the apparent width of the surface node, which is the only one we can measure, may be too small. Second, at the larger node widths a situation in which the capacitive transient becomes underdamped is being approached (see next section), the first indication of which is a shortening of the initial current surge. The demarcation line between the damped and underdamped response is not distinct and occurs at somewhat different node width to bundle diameters ratios in different preparations. Under such circumstances, it is not clear how the total apparent capacitance should behave.

At node widths greater than three or four preparation diameters, the initial downsweep of the capacitive transient becomes more rapid and a pronounced undershoot develops. Expanding the node still further leads to a ringing current pattern. This sequence is illustrated in Fig. 12 for a trabecula of 40 μm diameter. Small positive steps are illustrated; negative steps were symmetric.

These oscillations are expected from core conductor theory and from the sucrose gap voltage clamp configurations since one end of the test node is connected to the negative input of the control amplifier and the other end to the control amplifier output and there is a finite propagation lag across the preparation (c.f., Dodge and Frankenhaeuser, 1958; Johnson and Lieberman, 1971). In terms of sinusoidal analysis, the condition which gives rise to sustained oscillations is a loop amplification of 1 for a sinusoidal frequency which undergoes a 360° phase shift when passed through the control amplifier and the core conductor. Since the propagation lag increases with the increase of tissue length, one expects the observed decrease in ringing frequency shown in Fig. 12. What is most impressive about the data of Fig. 12 is the great length of test node that can be tolerated before oscillation sets in, in this case roughly five to six times the preparation diameter. This relation held approximately true over the range

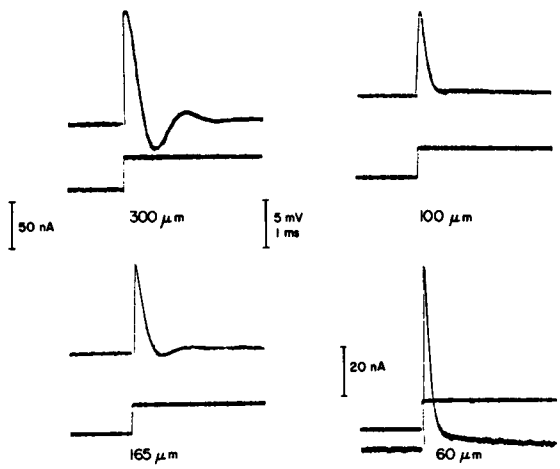

FIGURE 12 Changes in the capacitive transient of a 40 μm bundle as node is changed over a wide range. An increase in node width beyond 300 μm would have increased the number of oscillation cycles and slowed the frequency.

of preparations studied; that is, a thicker preparation could tolerate a wider node. The situation is certainly different from that in an axon where oscillatory behavior occurs when the test node is only slightly wider than the fiber diameter. An indication of this behavior in an axon appears in Fig. 10 in the work of Julian et al. (1962*b*).

The discrepancy in oscillatory lengths between axon and trabecula of the same outside dimensions is just the opposite of what one would expect, since a trabecula is composed of many small tubes and therefore has a very high capacitance to length ratio. The charging time for the core conductor is proportional to the specific membrane capacitance and to the sum of the internal and external resistivity and we would thus expect the minimum length for oscillation to be much shorter for a trabecula than for the axon of the same outer diameter. The larger series resistance of a trabecula is a stabilizing factor. To demonstrate this effect and to determine the approximate ringing frequencies one would expect, a ladder-network analog of a 50 μm diameter preparation was built (see inset, Fig. 13). Partial specifications are taken from the 50 μm preparation entry of Table I (6271). Each element of the ladder represents 20 μm of preparation. Values of C_m, R_m, and R_s were chosen so that the charge flow following a given voltage step and the ratios $(\Delta V_m/I_{leak}) = R_m$ and $\Delta V_m/I_{peak} = R_s$ were the

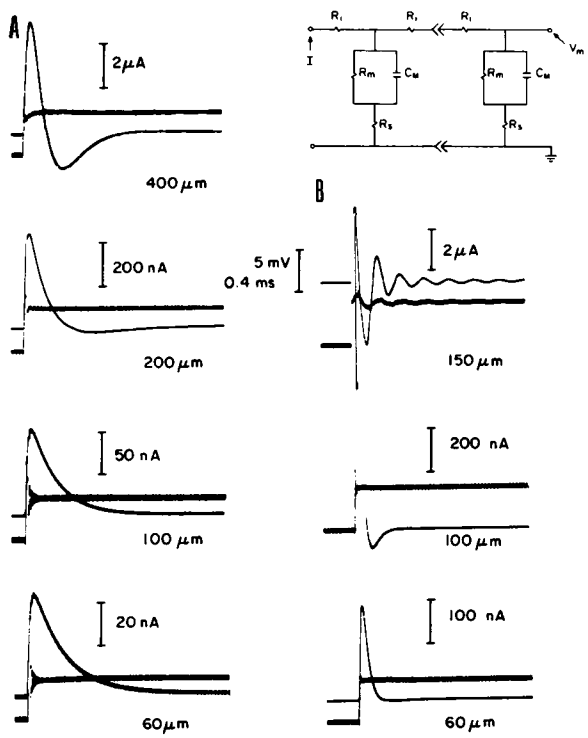

FIGURE 13 Transient response of the ladder network analog shown in the inset. One segment of analog represents 20 μm of preparation. *A*, response of various lengths of the analog with R_s = 250 kΩ. *B*, response with R_s = 50 kΩ. R_m = 6.8 MΩ; $C_m = 1.2 \times 10^{-9}$ F; R_i = 20 kΩ.

same for a 100 μm length of preparation and for the analog. Thus C_m was approximately 1/5 of the total measured capacitance and R_m was five times the leakage resistance. R_i was estimated by dividing the high frequency input resistance at the voltage pool by the length of tissue bathed by the sucrose collar. This method assumes that R_m is bypassed by C_m at both the end pool and test node and as before in this study that the extracellular current shunt can be neglected. This method and the assumption that the intracellular volume is the same as a single saline-filled tube gives a figure for internal resistivity of 200–400 Ω-cm. The analog employs R_i = 20 KΩ per section which corresponds to a resistivity of 200 Ω-cm. Fig. 13 *A* shows the response to a voltage step of the network representing 400, 200, 100, and 60 μm node widths. In Fig. 13 *B* R_s was reduced by a factor of 5 and the experiment repeated for node widths of 150, 100, and 60 μm. It is clear that a node of given width is less stable the smaller R_s is made; or conversely, increasing R_s increases stability.

The records of Fig. 13 exhibit qualitative similarities to records from actual preparations. For example, at the higher value of R_s (Fig. 13 *A*) the length at which the charging current becomes underdamped is approximately the same for preparation and analog. The ringing frequencies are also approximately the same. However, we do not consider this simple cable type of analog an adequate representation of the cable properties of the cardiac preparation. There are three major reasons for this. First, in the analog the capacitive decay at short node widths, < 150 μm, is indistinguishable from a single exponential. Second, the peak value of the charging transient is a much more sensitive function of node width in the analog than in the preparation. Third, for overly wide nodes the voltage at the sensing point can be controlled much more closely in the preparation than the analog.

A more reasonable approach to a model both in terms of electrical behavior and the gross tissue geometry is given in schematic form in Fig. 14. For illustration, a trabecula is shown broken into only two coaxial components, an annulus and an inner core of

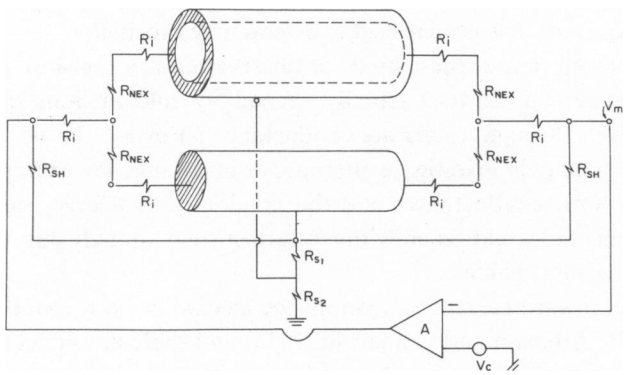

FIGURE 14 Coaxial model of a trabecula. External series resistances, R_{s_1}, R_{s_2}, are shown as lumped elements for illustration simplicity but are actually distributed elements. The R_i and R_{nex} elements are a voltage mixing network within the sucrose cuffs. R_{sh} represents an extracellular shunt path from the end pools to the test node.

cells each having a resistance, distributed between it and the external medium. A more complete description would include at least two annular components and a core. In the simplest, although not necessarily correct, geometric interpretation the inner core represents the inner cells of a bundle and would therefore have a relatively large series resistance which would be connected to an external ground via the smaller series resistance of the annulus, or outer cells. This type of model gives rise to anomalously long oscillatory lengths even with the series resistance of the outer cells made vanishingly small since the voltages at the ends of the two components (corresponding to the voltage pool side of the test node) are summed by a resistive network.

Analog simulations using the two line coaxial configuration of Fig. 14 have been performed to verify that the qualitative behavior of the model at different node widths corresponds to that of our preparation. Results are not included here since there are a sufficient number of unknowns in such a simulation, for example, the nature and influence of nexal interconnections, to make a separate study necessary to obtain a convincing quantitative fit of the oscillation data. Instead of analyzing a passive property, we have initially pursued the analysis of a single longitudinal section of the coaxial model and included Hodgkin-Huxley sodium channels (Hodgkin and Huxley, 1952) in order to provide a conceptual basis for the behavior of ion currents noted in this paper. The simulation would then correspond to a "short" node 50–100 μm width. Results of this study are presented in the following article (Jakobsson et al., 1975).

DISCUSSION

These experiments suggest strongly that, *in outline,* our cardiac muscle preparations seem to exhibit the same behavior as the classic axon model despite the confounding effects of the more complex geometry. In addition, many preparations displayed a slower inward current transient than is observed in axons. This current was greatly variable, but in all cases was much smaller than the rapid transient unless external calcium ion concentration was increased to several times normal.

The usual interpretation of these kinds of observations on the slow inward current has been to consider this current actually carried by calcium ions (and sometimes sodium ions as well) through a separate conductance pathway. To be sure, care must be exercised to adequately investigate alternatives involving, for example, control by calcium of other ionic conductances and the possibility that large, slow time-course spatial inhomogeneities could generate the inward current though slow gating of more or less standard sodium channels.

However, a net inward current in sodium-free media has been found here and elsewhere (Tarr, 1971; Aronson and Cranefield, 1973) and there are difficulties in imagining a net inward current carrier besides calcium under such circumstances. Likewise, action potentials (with a slow rate of rise) have been observed here and elsewhere in the absence of sodium. In the case of canine Purkinje fibers, the overshoot of the action potential and the rate of rise increase appropriate to a calcium mechanism when exter-

nal calcium is raised. Our data show a curious saturation of the peak slow inward current with increasing calcium and a rather small change in the "reversal potential." These data, however, should be viewed with the reservations discussed above held in mind.

Our analysis bears much similarity to the model of Kootsey and Johnson (1972) in its emphasis on the extracellular resistance. There is a considerable conceptual difference, however, in that the Kootsey and Johnson model formulates an extracellular space-clamp while in our scheme the bulk of the current injected at the current pool must pass across cell membranes. The critical parameter involved is the relative value of the resistance shunting the node membrane (R_{eg} from Fig. 1, Kootsey and Johnson, 1972). In our configuration, this resistance is large enough to reduce shunting current through the sucrose cuff to a value, negligible, with respect to the transmembrane current value. This conclusion is supported by two lines of evidence.

First, with regard to action potential amplitude, there is near equality of the transgap value and simultaneous microelectrode recording. Also, our transgap action potentials, when corrected for sucrose gap hyperpolarization, fall well within the range of published results. The customary circuit approximation for the sucrose gap is two parallel resistors representing internal and external longitudinal resistance through the sucrose region (c.f., Kootsey and Johnson, 1972; New and Trautwein, 1972). These resistances appear in Fig. 13 as ($R_i + R_{nex} + R_i = R_{int}$), internal resistance and R_{sh}, external. With this approximation, the transgap action potential should be attenuated by the factor ($R_{sh}/R_{sh} + R_{int}$) from its "true" or microelectrode-determined value. The attenuation as measured in our experimental configuration appears to be less than 10% as a conservative estimate; therefore, the shunt resistance is at least 10 times the internal resistance. To claim a much higher ratio than this, although it is quite probably so, would require more exacting and stable microelectrode recordings on small trabeculae than we have been able to make.

Second, a large number of trabeculae suffered stretch or crushing injury or partial termination along their length. In these instances, the transgap action potential was typically a small fraction—of the order of 25%—of normal size. When these preparations were tested in the chamber, the input resistance looking from the end pool nearer the injury site to ground (see Methods section) was very large, often 15–20 MΩ. The value for a healthy trabecula of 50 μM nominal diameter was around 2 MΩ. We would infer in these instances that internal current pathways were disrupted making R_{int} very large. The value of the parallel combination of R_{int} and R_{sh} which is the input resistance, would then increase toward its upper bound, i.e. toward R_{sh}, indicating that for this size of preparation R_{sh} in our gap was greater than 20 MΩ. It should be noted that, in general, even though the amplitude of the "transgap" action potential approaches that of an action potential recorded by a microelectrode, enough local current may flow to allow propagation past the gap. This is limited largely by R_{sh} since R_{sh} must be much larger than R_{int} before the APs approximate. Most experimenters put isotonic potassium chloride in the end pools to prevent such propagation. The fact

that we did not have to do this, leads us to believe our R_{sh}/R_{int} was quite a bit larger than the 10 to 1 ratio we have assumed.

There are experimental configurations in which the shunt current is clearly quite appreciable (c.f., New and Trautwein, 1972; Harrington and Johnson, 1973) and for which the extracellular space-clamp model would be more appropriate than the model used here.

It should be noted that using smaller trabeculae is desirable whichever model discussed is more appropriate. In fact, one of the paradoxes of the experimentation in this area is that larger bundles are more stable and often seem to have been preferred objects of study. Clearly, as muscle bundles are made smaller the sucrose can penetrate better. However, if a small enough bundle was used to assure a high extracellular resistance in the sucrose cuffs, the problems referred to by Kootsey and Johnson (aside from those emanating from a larger series resistance) would be relieved while the problems implied by our model would remain. What we have found here is that as the clamping became "somewhat" better "worse" behavior was exposed. The coaxial model was suggested as a step toward explaining that anomaly.

We would like to acknowledge the technical assistance of Burr Nelson, Susan Dragich, and Peter Carras in analyzing data and preparing the text figures.

This work was supported by U. S. Public Health Service grant HL 14125.

Received for publication 17 January 1975.

REFERENCES

ADRIAN, R. H., and W. ALMERS. 1974. Membrane capacity measurements on frog skeletal muscle in media of low ion content. *J. Physiol.* **237**:573.

ARONSON, R. S., and P. F. CRANEFIELD. 1973. The electrical activity of canine cardiac Purkinje fibers in sodium free, calcium rich solutions. *J. Gen. Physiol.* **61**:786.

BARR, L., M. DEWEY, and W. BERGER. 1965. Propagation of action potentials and the structure of the nexus in cardiac muscle. *J. Gen. Physiol.* **48**:797.

BEELER, G. W., and H. REUTER. 1970. Voltage clamp experiments on ventricular myocardial fibers. *J. Physiol.* **207**:165.

COLE, K. S. 1968. Membranes, Ions and Impulses. University of California Press, Berkeley.

CONNOR, J. A., E. JAKOBSSON, and L. BARR. 1973. Voltage clamp studies of frog atrial muscle. *Biophys. Soc. Annu. Meet. Abstr.* **13**:68*a*.

CONNOR, J. A., and C. F. STEVENS. 1971. Inward and delayed outward membrane currents in isolated neural somata under voltage clamp. *J. Physiol. (Lond.).* **213**:1.

CRANEFIELD, P. F., and B. F. HOFFMAN. 1958. Propagated repolarization in heart muscle. *J. Gen. Physiol.* **41**:633.

DODGE, F. A., and B. FRANKENHAEUSER. 1958. Membrane currents in isolated frog nerve fibre under voltage clamp conditions. *J. Physiol.* **143**:76–90.

FOZZARD, H. A. 1966. Membrane capacity of cardiac Purkinje fibre. *J. Physiol. (Lond.).* **182**:255.

GIEBISCH, G., and S. WEIDMANN. 1971. Membrane currents in mammalian ventricular heart muscle fibers using a voltage-clamp technique. *J. Gen. Physiol.* **57**:290.

GORMAN, A. L. F., and M. MIROLLI. 1972. The passive electrical properties of the membrane of a molluscan neurone. *J. Physiol.* **227**:35.

HAAS, H. G., R. KERN, H. M. EINWACHTER, and M. TARR. 1971. Kinetics of Na inactivation in frog atria. *Pfluegers Arch. Gesamte Physiol.* **323**:141.

HARRINGTON, L., and E. A. JOHNSON. 1973. Voltage clamp of cardiac muscles in a double sucrose gap. *Biophys. J.* **13**:626.

HILLE, B. 1968. Pharmacological modifications of the Na channel of frog nerves. *J. Gen. Physiol.* **51**:199.

HODGKIN, A. L., and A. F. HUXLEY. 1952. A quantitative description of membrane current and its application to conduction and excitation in nerve. *J. Physiol.* **117**:500.

HUTTER, O. F., and W. TRAUTWEIN. 1956. Vagal and sympathetic effects on the pacemaker fibers in the sinus venosus of the heart. *J. Gen. Physiol.* **39**:715.

JAKOBSSON, E., L. BARR, and J. A. CONNOR. 1975. An equivalent circuit for small atrial trabeculae of frog. *Biophys. J.* **15**:1069.

JAKOBSSON, E., J. A. CONNOR, and L. BARR. 1974. A simulation of voltage clamp experiments on frog atrial trabeculae. *Fed. Proc.* **33**:1012.

JOHNSON, E. A., and M. LIEBERMAN. 1971. Heart: excitation and contraction. *Ann. Rev. Physiol.* **33**:479.

JULIAN, F. J., J. W. MOORE, and D. E. GOLDMAN. 1962 *a*. Membrane potentials of the lobster giant axon obtained by use of the sucrose-gap technique. *J. Gen. Physiol.* **45**:1195.

JULIAN, F. J., J. W. MOORE, and D. E. GOLDMAN. 1962 *b*. Current-voltage relations in the lobster giant axon membrane under voltage clamp conditions. *J. Gen. Physiol.* **45**:1217.

KOOTSEY, J. M., and E. JOHNSON. 1972. Voltage clamp of cardiac muscle. *Biophys. J.* **12**:1496.

NAKAJIMA, S., and J. BASTIAN. 1974. Double sucrose gap method applied to single muscle fiber of *Xenopus laevis*. *J. Gen. Physiol.* **63**:235.

NARAHASHI, T., J. W. MOORE, and W. R. SCOTT. 1964. Tetrodotoxin blockage of sodium conductance increase in lobster giant axons. *J. Gen. Physiol.* **47**:965.

NEW, W., and W. TRAUTWEIN. 1972. Inward membrane currents in myocardial muscle fibres. *Pfluegers Arch. Gesamte Physiol.* **334**:1.

ROUGIER, O., G. VASSORT, D. GARNIER, Y. M. GARGOUIL, and E. CORABOEUF. 1969. Existence and role of a slow inward current during the frog atrial action potential. *Pfluegers Arch. Gesamte Physiol.* **308**:91.

ROUGIER, O., G. VASSORT, and R. STÄMPFLI. 1968. Voltage clamp experiments on frog atrial heart muscle with the double sucrose gap technique. *Pfluegers Arch. Gesamte Physiol.* **301**:91.

STALEY, N. A., and E. S. BENSON. 1968. The ultrastructure of frog ventricular cardiac muscle and its relationship to mechanisms of excitation-contraction coupling. *J. Cell. Biol.* **38**:99.

TARR, M. 1971. Two inward currents in frog atrial muscle. *J. Gen. Physiol.* **51**:523.

TARR, M., and J. TRANK. 1971. Equivalent circuit of frog atrial tissue as determined by voltage clamp-unclamp experiments. *J. Gen. Physiol.* **58**:511.

TAYLOR, R. E., J. W. MOORE, and K. S. COLE. 1960. Analysis of certain errors in squid axon voltage clamp measurements. *Biophys. J.* **1**:161.